Sequence-Dependent Drug Binding to the Minor Groove of DNA: Crystal Structure of the DNA Dodecamer d(CGCAAATTTGCG)$_2$ Complexed with Propamidine

Christine M. Nunn and Stephen Neidle*

CRC Biomolecular Structure Unit, The Institute of Cancer Research, Sutton, Surrey SM2 5NG, U.K.

Received February 6, 1995[⊗]

The DNA-binding ligand propamidine, an analogue of the drug pentamidine which is used in the treatment of acquired immune deficiency syndrome (AIDS)-associated *Pneumocystis carinii*, has been cocrystallized with the DNA sequence d(CGCAAATTTGCG)$_2$, and the crystal structure of the complex has been determined using data from 8 to 2.2 Å resolution. The *R* factor converged to 15.5% with the inclusion of 73 water molecules. The structure shows binding of the propamidine molecule within the AT tract of the DNA minor groove with a shift from the center of the duplex toward the 3′ end of ca. 2 Å. The long AT tract of six base pairs in length allows the propamidine many potential binding sites in the DNA groove, and its binding is seen to occur where there is least perturbation to the DNA from that seen in the native structure. The interactions with bases are distinct from those previously observed for the sequence d(CGCGAATTCGCG)$_2$.

Introduction

The interaction of drugs such as netropsin, distamycin, and berenil with DNA occurs, in large part, at AT-rich regions of DNA.[1] Crystallographic studies in particular have shown that drug binding occurs in the narrow minor groove of B-form duplexes.[2] The interactions between drug and DNA involve hydrogen bonding from donor groups on the drug to acceptor groups on the DNA bases. In addition, van der Waals contacts occur between the drug molecule and the atoms which form the walls of the DNA minor groove. The pattern of these close contacts can follow the convex curvature of the minor groove; optimal drug fit has been termed "isohelicity".[3] The question of the relative importance of these two factors, hydrogen bonding and van der Waals contacts, for directing a drug to a particular DNA sequence remains unresolved, as is the importance of DNA perturbation. The definition of a drug–DNA sequence recognition code analogous to those proposed for protein–DNA recognition[4] remains elusive. In spite of this, many minor groove-binding ligands have been designed and synthesized on the basis of information gained from crystallographic and NMR structure analyses.[5]

The DNA minor groove is also the locus for a number of DNA-binding proteins, some of which are involved in gene regulation. These include the homeodomain family[6] and the TATA box protein[7] which binds within the minor groove and bends the sequence 5′-TATA. Some proteins such as the HMG chromosomal proteins bind exclusively within the minor groove,[8] whereas the bacterial recombination enzyme Hin recombinase binds to DNA in both the minor and major grooves.[9] It is possible that the mechanisms of biological action of the minor groove-binding drugs involve direct interference with protein–DNA minor groove recognition. This is indicated in the finding that distamycin can compete for protein in homeodomain–DNA complexes[10] and for several minor groove-binding drugs which interact with the TATA box-binding protein–DNA complex.[11]

Propamidine, 1,3-bis(4-amidinophenoxy)propane (Figure 1), is a short chain homologue of pentamidine, 1,5-bis(4-amidinophenoxy)pentane, a drug which is active against the *Pneumocystis carinii* pathogen. Pentamidine has been widely used in the treatment of *P. carinii* pneumonia (PCP), the opportunistic infection which occurs in the majority of acquired immune

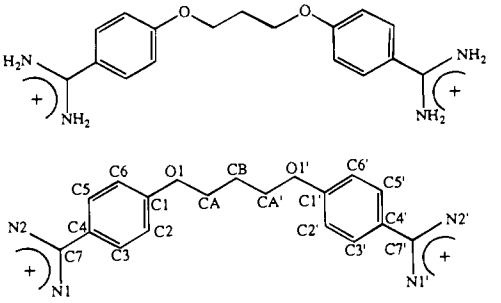

Figure 1. Structure of propamidine, together with the atomic numbering scheme.

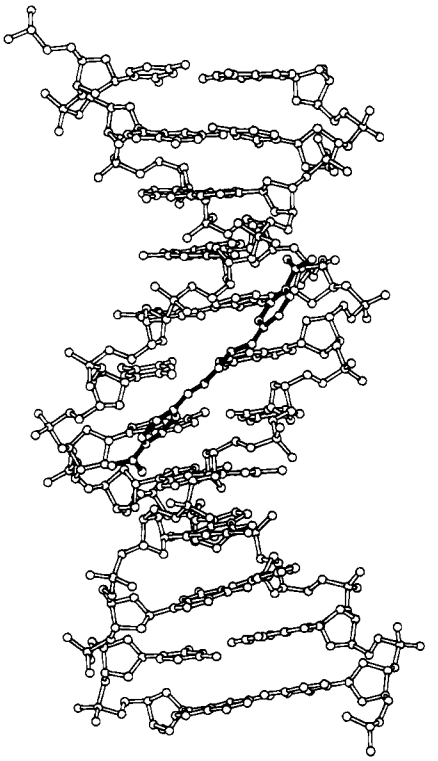

Figure 2. View of the propamidine–d(CGCAAATTTGCG)$_2$ complex.

* To whom correspondence should be addressed.

[⊗] Abstract published in *Advance ACS Abstracts*, May 1, 1995.

0022-2623/95/1838-2317$09.00/0

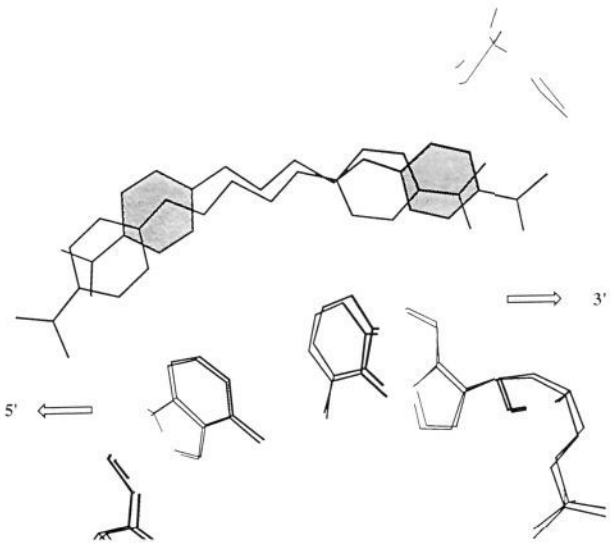

Figure 3. Overlay of the DNA structures for d(CGCAAATTTGCG)$_2$ and d(CGCGAATTCGCG)$_2$ after binding to propamidine, viewed toward the plane of the propamidine phenyl rings. The propamidine–d(CGCAAATTTGCG)$_2$ phenyl rings are shown in stiple.

deficiency syndrome (AIDS) patients.[12] The mechanism of pentamidine action against *P. carinii* is unknown, however, there is considerable evidence to suggest that direct interaction with the pathogenic genome is important for its activity.[13] Associated with the use of pentamidine in the clinic are a number of toxic side effects, and studies are underway to find and investigate improved linked bis(amidine) analogues with diminished toxicity and greater efficacy. To this end we are investigating by means of X-ray crystallography how pentamidine and some of its analogues interact with DNA.

X-ray crystal structure determinations have been carried out in our laboratory for both pentamidine and propamidine bound to the DNA sequence d(CGCGAATTCGCG)$_2$.[14] This sequence (to be termed A2T2 in this paper) was chosen due to the very stable packing arrangement of this structure, which involves interduplex hydrogen-bonding interactions of the type N–H···N between guanine bases across the DNA minor groove.[15] For both structures, binding of the ligand occurs within the stable AT-rich region of the DNA minor groove, as had been previously suggested for pentamidine from footprinting studies.[16] From an examination of these two structures, we have been able to establish a rationale for the superior binding ability of propamidine as compared with pentamidine.[14b] These results have agreed with, and extended, previous experimental evidence obtained from thermal denaturation measurements and molecular modeling studies.[3c,17]

This paper reports the crystal structure of propamidine bound to the DNA sequence d(CGCAAATTTGCG)$_2$ (to be termed A3T3 in this paper) and thus examines the effects of propamidine binding to a DNA sequence with a six-base pair AT tract, which contains a number of potential drug-binding sites. The DNA sequence d(CGCAAATTTGCG)$_2$ has a similar crystal packing arrangement to that seen for d(CGCGAATTCGCG)$_2$ with the central AT base pairs remote from the effects of crystal packing and presenting a stable template for ligand binding.[14a] A number of crystal structure determinations using this DNA sequence have previously been carried out for the minor groove-binding ligands berenil,[2d] distamycin,[18] netropsin,[2c] and Hoechst 33258.[19]

Results

The crystal structure shows a propamidine molecule bound to the DNA duplex within the AT region of the minor groove (Figure 2). It is apparent that the position for the ligand is quite distinct from that found for the propamidine ligand in its complex with the A2T2 sequence,[14b] where the ligand was symmetrically bound within the DNA minor groove. Figure 3 shows an overlay of the DNA in the two structures to illustrate the position of the two propamidine molecules with respect to one another. The ligand lies displaced in the present structure from the center of the DNA duplex with a shift of ca. 2 Å toward the 3′ end of strand 1 in the duplex, compared with its position in the A2T2 complex. The relative displacement of the two ligands is shown in Figure 4 viewed toward the minor groove.

Drug–DNA Binding and Propamidine Conformation. The protonated amidinium groups of the propamidine molecule are involved in both direct and

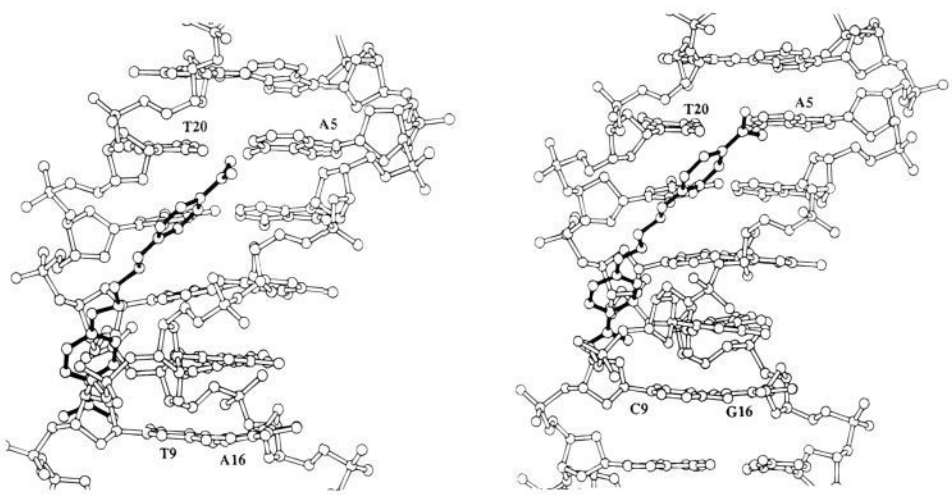

(a) **(b)**

Figure 4. View of the propamidine position within the minor groove for propamidine binding to (a) d(CGCAAATTTGCG)$_2$ and (b) (CGCGAATTCGCG)$_2$.

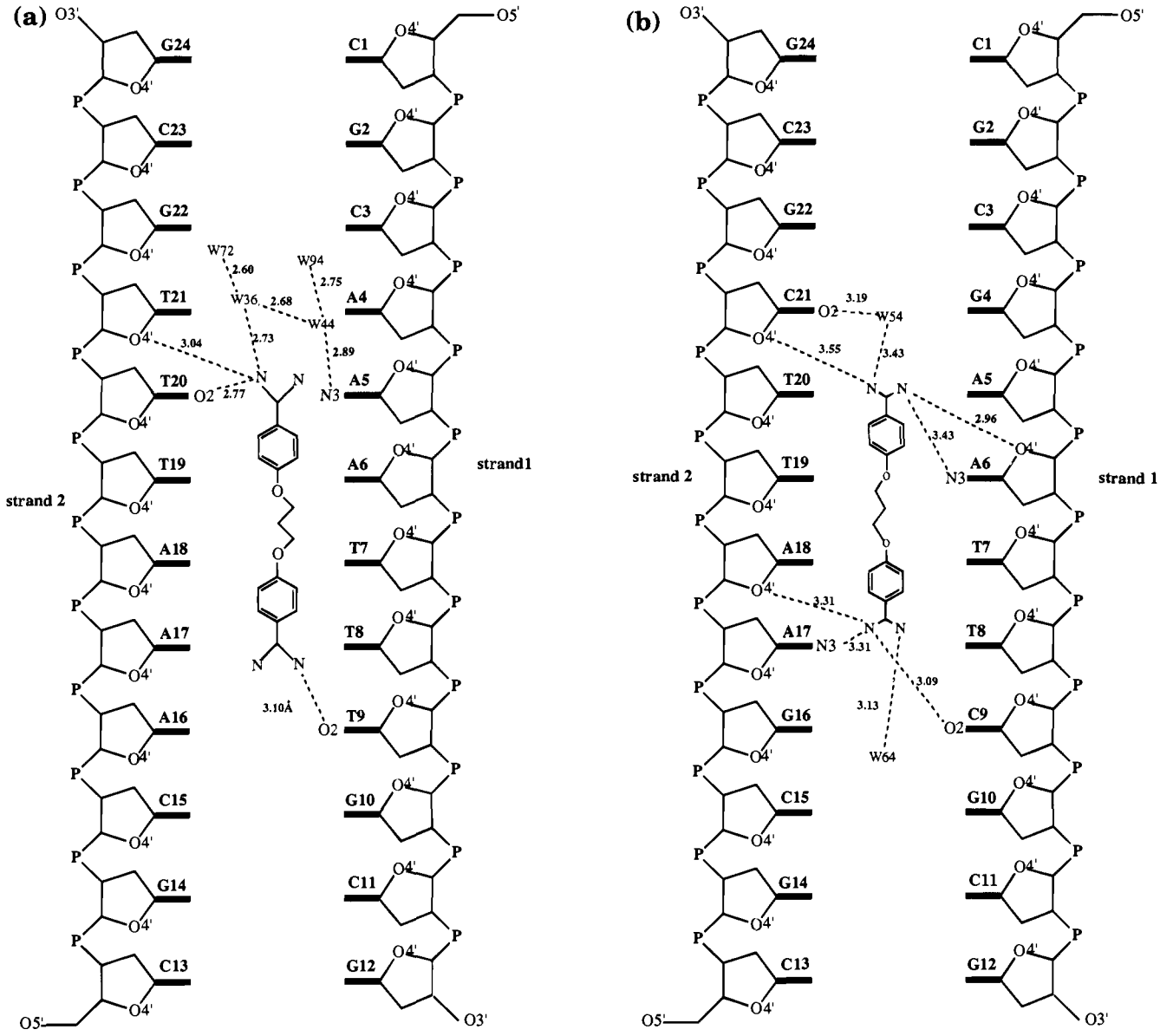

Figure 5. Schematic representation of the hydrogen-bonding interactions between propamidine and (a) the d(CGCAAATTTGCG)$_2$ sequence and (b) the d(CGCGAATTCGCG)$_2$ sequence. **P** represents the CH_2PO_4-group.

indirect hydrogen-bonding interactions with the DNA bases and deoxyribose sugar groups. At one end of the drug, only one hydrogen bond is observed between one of the amidinium groups of the propamidine ligand and the O2 atom of Thy 9. At the other end, one amidinium group hydrogen bonds with the O4′ atom of the deoxyribose group of Thy 21 as well as with atom O2 of Thy 20. In addition a solvent-mediated hydrogen bond occurs with atom N3 of Ade 5, via water molecules W36 and W44. These interactions are shown schematically in Figure 5 together with those previously observed for the structure of propamidine bound to A2T2.[14b] We observe an equivalent interaction at the 3′ end of the propamidine molecule in both structures from one amidinium group to the O2 atom of either Thy 9 (A3T3) or Cyt 9 (A2T2). For the A2T2 complex, there is also an additional interaction at this end of the drug, from the other amidinium group to atoms N3 of Ade 17 and the O4′ sugar atom attached to base Ade 18. At the other end of the propamidine ligand, we observe quite distinct differences in DNA interactions. For the A2T2 complex, a solvent-mediated interaction occurs from one amidinium group to the O2 atom of Cyt 21, in contrast to the direct interaction in the A3T3 complex to atom O2 of Thy 20. The direct interactions seen in the A2T2 complex for the second amidinium group with the O4′ atom of the sugar group attached to Ade 6 and atom N3 of Ade 6 are not observed in the A3T3 complex. Atoms O2 of Thy 9 in A3T3 and Cyt 9 in A2T2 both hydrogen bond to a propamidine amidinium group; however, the distance between these two amidinium groups is 2.6 Å. The differences in the interactions seen at the 5′ end of the two complexes are a result of the propamidine ligand being displaced from the center of the duplex toward the 3′ end of the A3T3 sequence. The amidinium groups of the propamidine ligand in the case of the A3T3 complex are close to the O2 atom of Thy 20, whereas in the A2T2 complex the propamidine ligands extends further in the 5′ direction and makes a solvent-mediated interaction with atom O2 of Thy 21.

The propamidine molecule makes contact with the DNA minor groove via the phenyl hydrogen atoms and

Figure 6. Fitting of the propamidine ligand within the molecular surface of the DNA minor groove after binding to d(CGCAAATTTGCG)$_2$ and d(CGCGAATTCGCG)$_2$. Figures were calculated using the program GRASP.[26] Surface colors range from 0 (red) to 5 (white) Å for distance between groove surface and ligand atom center.

those attached to the -$(CH_2)_3$- linker which lie in close contact with the atoms that line the floor and walls of the DNA minor groove. Figure 6 displays the DNA minor groove molecular surface for the propamidine–A3T3 and propamidine–A2T2 complexes and illustrates the fitting of the two propamidine ligands within the groove surface of their associated DNA sequences. In both complexes the propamidine molecule is nonplanar and twisted along the central dioxyalkane linkage of the molecule as well as at the terminal amidinium groups. This flexibility enables the ligand to match the pitch of the DNA helix which results in a good isohelical fit[3a] to the minor groove. The two propamidine molecules in the complexes differ in their -$CO(CH_2)_3OC$- torsion angles, with values for the A3T3 (and A2T2) complexes of (C1–O1–CA–CB) −170° (−178°), (O1–CA–CB–CA′) −155° (−166°), (CA–CB–CA′–O1′) −164° (−170°), and (CB–CA′–O1′–C1′) −176° (−171°). In the A3T3 complex the two aromatic rings of the propamidine are twisted by 34° with respect to each other, as compared with 30° in the A2T2 complex, with the dihedral angle between the phenyl rings and their neighboring amidinium planes being 14° and 26° for C7–N1–N2 and C7′–N1′–N2′, respectively, as compared to 7° and 17° in the A2T2 complex. The twisting observed for propamidine in this structure is thus greater than seen for the propamidine ligand when bound to A2T2.

Influence of Propamidine on DNA Conformation. Upon binding of the propamidine to the A3T3 sequence, we observe small ligand-induced changes in DNA conformation throughout the entire structure, compared with those found in the native A3T3 structure.[14a] Helical parameters for propamidine complexed with A3T3 and A2T2 together with the two native sequences are shown in Figure 7. No major changes in base–base geometry or DNA conformation appear to result from propamidine binding to the A3T3 sequence, with a total rms deviation between the DNA of 0.39 Å in the propamidine-bound and native A3T3 structures. Comparing the helical parameters for the DNA dodecamer sequence A2T2 after binding to propamidine with the title complex, the most marked differences in base morphology are seen for the increased buckle at the first A-T base pair A4:T21 and the increased cup at the CpA and TpG base steps C3pA4 and T9pG10 in the A3T3 sequence. Differences also occur in the roll values at step 4 where the propamidine–A2T2 complex opens toward the minor groove.

The rms deviation between the A3T3 and A2T2 sequences in their propamidine-bound structures is 1.42 Å. Figure 8 shows a plot of the minor groove width for the propamidine–A3T3 complex, together with the native A3T3 structure[14a] and the propamidine–A2T2 complex.[14b] It can be seen that the native A3T3 DNA sequence, which has the minor groove filled by a ribbon of hydration,[14a] is virtually unchanged as a result of propamidine binding and displays an almost identical minor groove width to that of the propamidine-bound complex. This is in apparent contrast to what was observed for the propamidine–A2T2 structure,[14b] in which the minor groove shows appreciable widening upon ligand binding. Even so, comparing the groove width of propamidine–A3T3 with propamidine–A2T2, the DNA sequence with the longer AT tract shows the narrower groove width with bound propamidine.

In the central AT tract of the duplex for both the native and propamidine-bound A3T3 sequences, we observe in addition to the usual Watson–Crick A:T base

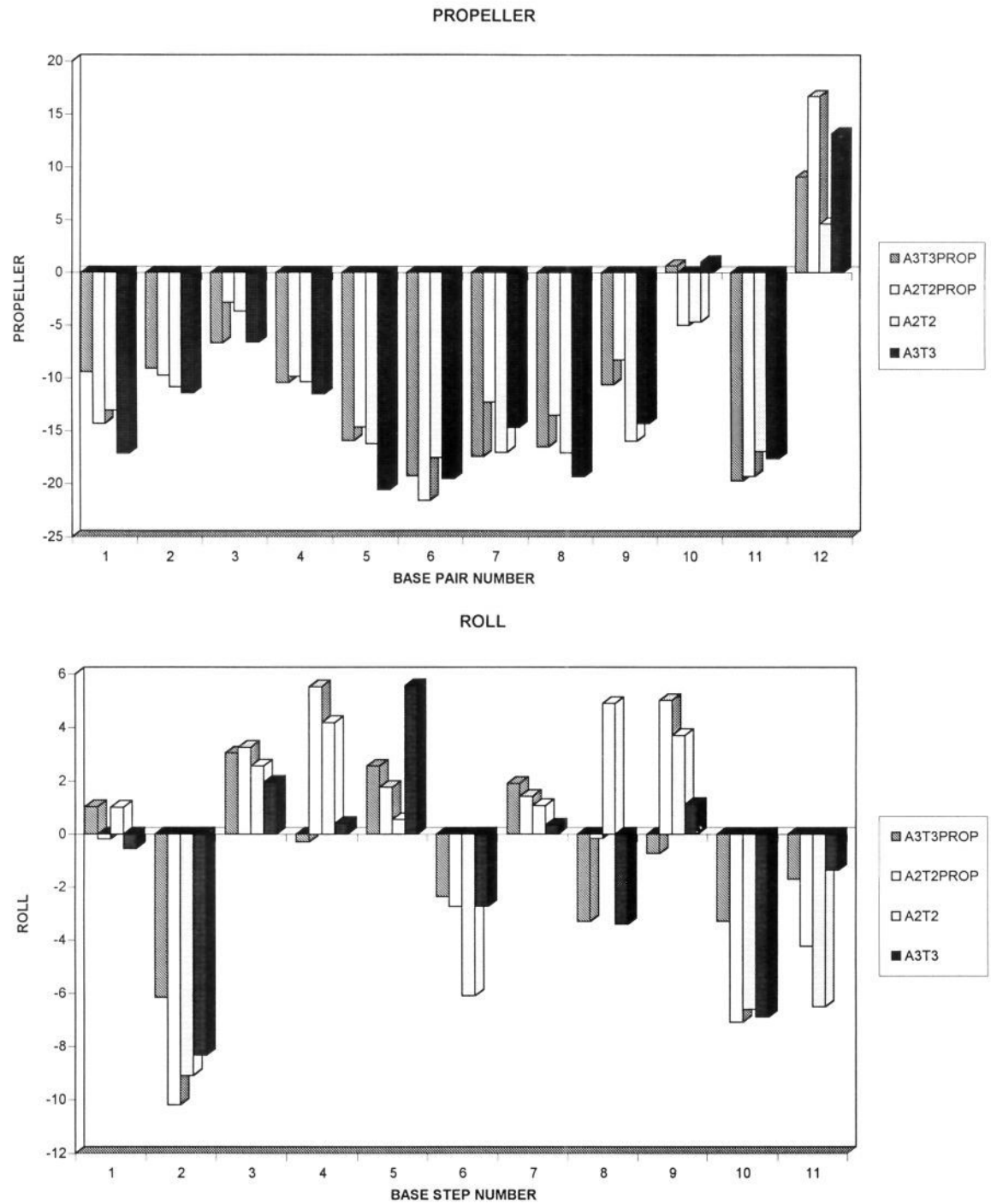

Figure 7. Selected helical parameters for the DNA in the propamidine–d(CGCAAATTTGCG)$_2$ complex together with the propamidine–d(CGCGAATTCGCG)$_2$ complex and the two native structures, calculated using the NEWHEL92 program.

pairing a major groove hydrogen-bonding interaction from atom N6 of Ade 5 to atom O4 of Thy 19. The distances involved are 3.2 and 3.1 Å for the propamidine complex and native DNA, respectively. A longer interaction of 3.2 Å also exists between atom N6 of Ade 17 and atom O4 of Thy 7 in the propamidine-bound complex. Similar three-center or bifurcated hydrogen bonding has been observed in a number of AT-rich DNA dodecamers including the structures of netropsin and distamycin bound to the A3T3 sequence[18,2c] where the interactions are more extensive than observed here. These interactions result from the high propellor twists that are observed for the region of A:T base pairing in these structures. For berenil bound to A3T3,[2d] no three-center hydrogen bonding was observed.

Hydration. A total of 73 water molecules were located in the structure. The first hydration shell waters are involved in hydrogen bonding to the DNA phosphate oxygen atoms, base functional groups, and oxygen atoms of the sugar groups and phosphodiester backbone. A novel hydration network was found to occur in the structures of propamidine and γ-oxapentamidine bound to the A2T2 sequence.[14b,20] This hydration network was seen to run along the full length of the minor groove, following the exterior edge of the minor groove binding molecule. A similar "hydrophobic

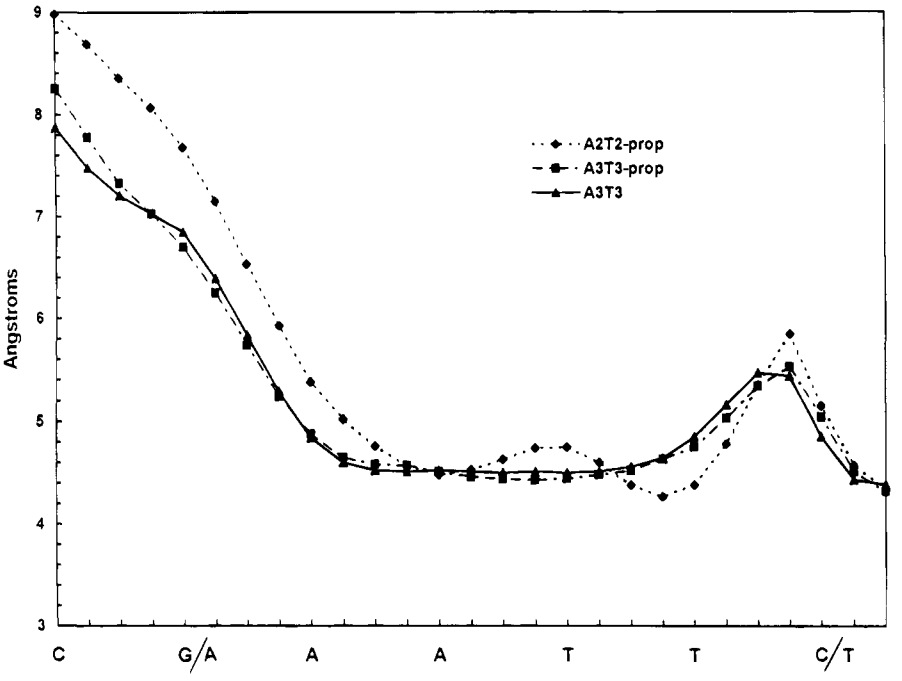

Figure 8. Minor groove width for the propamidine–d(CGCAAATTTGCG)$_2$ complex (prop–A3T3), the propamidine–d(CGCGAATTCGCG)$_2$ complex (prop–A2T2), and the native A3T3 structure, calculated using the program CURVES.[27]

spine of hydration" was not seen in this complex and is possibly a feature of ligand binding specifically to the DNA sequence d(CGCGAATTCGCG)$_2$.

Discussion

The propamidine ligand is found to interact with the DNA sequence d(CGCAAATTTGCG)$_2$ by classic minor groove binding via interactions within the AT-rich region of the DNA minor groove involving a combination of hydrogen bonding and van der Waals close contacts. Two structure determinations have now been carried out with the propamidine ligand bound to DNA sequences. It is of interest to consider the title complex in light of the previously determined structure of propamidine bound to d(CGCGAATTCGCG)$_2$[14b] and compare the features of DNA recognition seen for propamidine bound to these two slightly different DNA sequences.

DNA Recognition. The position of the propamidine ligand within the DNA minor groove of d(CGCAAATTTGCG)$_2$ is well defined by the electron density (Figure 9) and shows no positional disorder along the length of the groove. The propamidine lies displaced toward the 3′ end of the DNA upon binding and differs from the symmetric binding previously seen for propamidine bound to d(CGCGAATTCGCG)$_2$.[14b] This difference of about 2 Å in groove position of the propamidine ligand in the two complexes results in a different pattern of hydrogen-bonding interactions between the propamidine and the DNA in the two structures. The number of hydrogen-bonding interactions observed for propamidine bound to A3T3 is less than was observed the A2T2 complex, with three strong direct hydrogen-bonding interactions occurring from the propamidine amidinium groups to two thymine O2 atoms and one sugar O4′ atom. This compares with four interactions of 3.3 Å or less in the case of the A2T2 complex, with in addition two weaker interactions from the amidinium groups to N3 of Ade 6 and the O4′ atom of the sugar

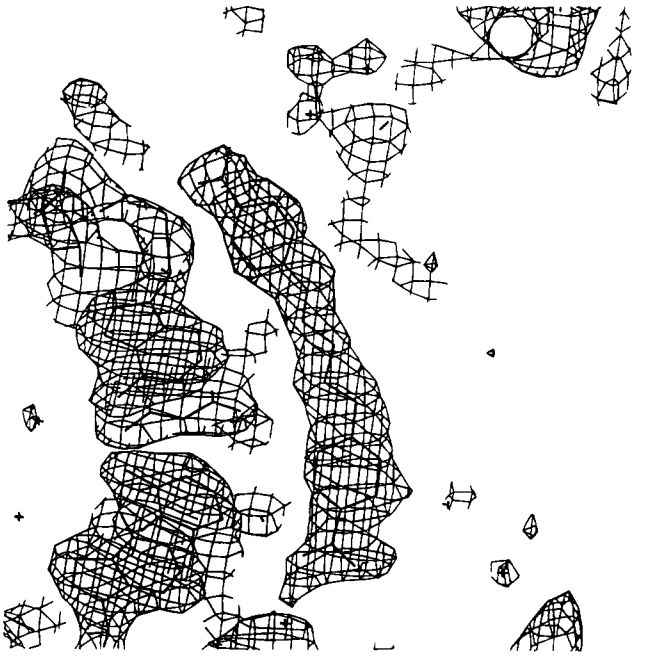

Figure 9. $2F_o - F_c$ map (1σ level) of the propamidine ligand within the DNA minor groove, calculated at the end of the refinement.

attached to Cyt 21. Thus, the driving force for the shift in ligand position when propamidine binds to A3T3 vs A2T2 cannot be explained in terms of increased hydrogen-bonding interactions between the ligand and the DNA. The two distinct patterns of hydrogen bonding seen for these two structures are of potential significance in the rational design of new pentamidine analogues and minor groove-binding ligands in general. The results of these two crystal structures show that different DNA sequences recognize a given minor groove-binding ligand in distinctive ways.

Upon binding of propamidine to A3T3 there is little effect upon the structure of the DNA. This is well

illustrated by the helical parameters (Figure 7) and the minor groove geometry (Figure 8). From this evidence we suggest that the ligand assumes a position in the A3T3 minor groove which results in the least perturbation to the DNA structure and that this is the overriding factor in determining the position of the ligand upon binding to DNA. For the A3T3 compared to A2T2 structures, the longer length of the AT tract allows for a greater number of potential ligand-binding sites and more possibility for the ligand to assume a favorable fit within the groove.

As shown in Figure 6, the propamidine molecule is seen to fit well into the minor groove surface of both the A3T3 and A2T2 sequences, with twisting of the ligand occurring to effect a snug fit between the propamidine molecule and the DNA. The difference in degree of ligand twisting probably reflects the different groove geometry of the two DNA sequences, with the widened groove width of the A2T2 structure requiring less twisting of the propamidine to effect a good fit within the groove. The reduced width of the minor groove for A3T3 as compared with A2T2 results in more extensive van der Waals contacts between the propamidine and the DNA minor groove surface of this complex.

Implications for Drug Design. The majority of noncovalent minor groove ligand design studies to date has focused on improvements to DNA binding affinity and achieving GC as well as AT sequence recognition. There has been recent success in the design of dimer motifs that achieve mixed-sequence recognition of predefined target sequences utilizing the concept of dimeric molecules fitting a widened minor groove, together with direct hydrogen-bonding base recognition.[5a,c] The present results imply that it is necessary to consider the *geometric features of the exact target sequence and that* closely related sequences may show different features of recognition. Major differences in ligand position as observed here can occur for just a small change in DNA sequence.

Propamidine and DNA Mobility. In addition to the determination of atomic positions within the unit cell, an X-ray crystal structure determination provides information about the mean square displacements of the individual atoms within the structure. This displacement can be considered as representing the degree of vibration or movement of an atom within the structure, as well as dynamic disorder. From the atomic thermal parameters obtained for each atom in the structure, a qualitative measure of the atomic mobility can be gained. For DNA structures, we observe different atomic thermal motion for different regions of the molecule, with the degree of thermal motion of the substituent groups increasing in the order bases < sugars < phosphates. For the propamidine–DNA complexes and associated pentamidine–A2T2 and γ-oxapentamidine–A2T2 complexes, we have compared the thermal mobility seen for the ligand atoms within the complexes to learn about the degree of motion and indirectly about the strength of DNA-binding for these ligands.

Figure 10 shows a plot of the mean atomic thermal motion for the base, sugar, and phosphate groups in the DNA duplexes A2T2 and A3T3 and also for the ligand molecules within the complexes. In the case of the propamidine bound structures, the crystal structure determinations were carried out at 289 K, and for both structures, the propamidine ligand atoms show greater mobility than their associated DNA atoms. There is an overall reduction in mobility over the entire structure for propamidine–A3T3 as compared with propamidine–A2T2, with no significant difference observed for the thermal motion of the propamidine ligand within these two complexes, with mean values of 34.3 and 38.8 Å^2 for the A3T3 and A2T2 complexes, respectively.

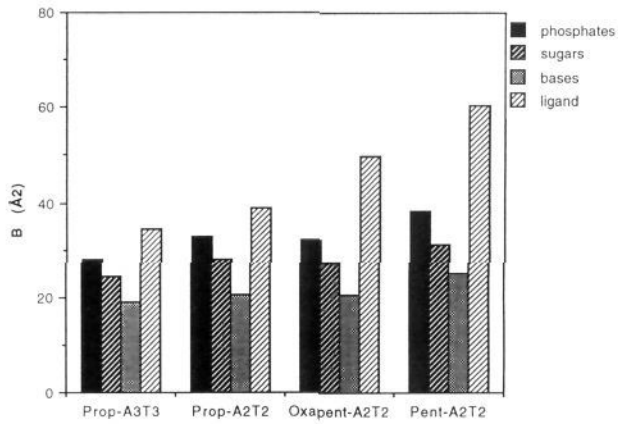

Figure 10. Plot showing the mean thermal parameters (Å^2) for regions of the propamidine–d(CGCAAATTTGCG)$_2$ complex together with the complexes with propamidine, γ-oxapentamidine, and pentamidine bound to the d(CGCGAATTCGCG)$_2$ sequence.

It is interesting to compare propamidine mobility upon DNA minor groove binding with that of the closely analogous γ-oxapentamidine and pentamidine ligands. The recently determined crystal structure of γ-oxapentamidine–A2T2[20] shows very similar values for the DNA *atoms with increased mobility for the γ-oxa*pentamidine ligand (mean value 49.9 Å^2), as compared to propamidine. For the pentamidine–A2T2 structure,[14a] the entire structure shows increased mobility with the mean value for the pentamidine ligand of 60.3 Å^2.

Experimental Section

Synthesis and Crystallization. The DNA dodecamer d(CGCAAATTTGCG) was purchased from Oswel DNA Service (University of Edinburgh, Edinburgh, Scotland, U.K.) and annealed before use. Propamidine was synthesized in this laboratory by Dr. T. C. Jenkins as the dihydrochloride salt. Crystals were grown from sitting drops at 277 K containing 5 μL of 3 mM DNA, 5 μL of 100 mM $MgCl_2$, 4 μL of 15 mM propamidine, and 5 μL of 45% 2-methylpentane-2,4-diol (MPD), equilibrated against a reservoir containing 2 mL of 45% MPD. All of the solutions were prepared using 30 mM sodium cacodylate buffer, pH 7.0, and added together in the order listed to prevent drug precipitation. Colorless rhomb-shaped X-ray quality crystals were obtained after about 3 weeks.

Data Collection. Intensity data were collected at 289 K using a Siemens-Xentronics multiwire area detector equipped with a rotating anode X-ray generator (40 mA, 70 kV) and graphite monochromator. A crystal-to-detector distance of 10 cm and a swing angle of 15° were used to collect data to a resolution of 2.2 Å. Data were collected with χ set at 45° and values of φ fixed at 260°, 320°, and 200°. The crystal was rotated through 100° in ω for φ = 260° and 320° and through 50° for φ = 200°; 180 s frames were recorded every 0.2° step. No crystal decay occurred during the data collection.

Data processing was carried out using the program package XENGEN, version 1.3. A total of 12 110 out of a possible 12 997 reflections were collected and merged to give 3410 of the 3757 possible unique reflections (90.8%) to 2.2 Å resolution

with a merging R value of 5.3%; 2341 of these reflections were observed at the $2\sigma(F)$ level.

Structure Solution and Crystallographic Refinement. The unit cell dimensions of the crystal are a = 24.78 Å, b = 41.16 Å, and c = 65.51 Å, in the orthorhombic space group $P2_12_12_1$. This cell is close to that for the native dodecamer sequence reported by Edwards *et al.*[14a] (a = 24.87 Å, b = 40.90 Å, and c = 65.64 Å) and Coll *et al.*[18] (a) = 25.20 Å, b = 41.65 Å, and c = 65.81 Å), suggesting an isomorphous structure. The coordinate file for the native dodecamer sequence reported by Edwards *et al.* was obtained from the Nucleic Acid Database[21] and used as a starting model for the structure refinement.

The model was initially refined by rigid body refinement with one constrained group for data from 8 to 3.5 Å (842 reflections) using the program X-PLOR.[22] The R value decreased to 27.9%. The DNA was then divided into 24 rigid groups, and the resolution range of the data used for refinement increased from 8–3.5 Å (R = 24.3%) to 8–2.2 Å (R = 25.7%). Crystallographic refinement continued with conventional positional refinement using conjugate gradient energy minimization for all data from 8 to 2.2 Å resolution. Following 120 cycles of refinement, the R factor was 22.8%. Refinement of the atomic temperature factors reduced the R factor further to 21.7%. Electron density maps were calculated and displayed using the graphics package 'O' version 5.7.[23] $F_o - F_c$ maps show a discrete elongated lobe of density visible at this stage lying within the minor groove of the DNA. A molecule of propamidine was manually fitted into this density, and refinement of the DNA and propamidine continued using conjugate gradient positional refinement and atomic temperature factor refinement. Propamidine electrostatic charges were calculated using MNDO wave functions,[24] and the force field parameters were interpolated from molecular modeling studies carried out in this laboratory.[25] During the course of the refinement, the drug molecule was refitted and solvent positions were included, being assigned as water molecules.

At the end of the refinement a total of 73 water atoms were included to give a final R value of 15.5%, for all data in the range 8–2.2 Å. The root-mean-square deviations from target values are 0.022 Å for the bond lengths and 4.0° for bond angles. The X-PLOR refinement and the R factor calculations used $F > 2\sigma$ data. Final refined coordinates, together with observed and calculated structure factors, have been deposited in the Brookhaven Protein Data Bank (identification code 102D) and the Nucleic Acid Database.

Acknowledgment. We wish to thank Terry Jenkins for supplying the propamidine sample and the Cancer Research Campaign for financial support.

References

(1) (a) Dervan, P. B. Design of Sequence-Specific DNA-Binding Molecules. *Science* **1986**, *232*, 464–471. (b) Kopka, M. L.; Larsen, T. A. Netropsin and the Lexitropsins. The Search for Sequence-Specific Minor-Groove-Binding Ligands. In *Nucleic Acid Targeted Drug Design*; Propst, C. L., Perun, T. J., Eds.; Marcel Dekker, Inc.: New York, 1992; pp 302–374.

(2) (a) Kopka, M. L.; Yoon, C.; Goodsell, D.; Pjura, P.; Dickerson, R. E. The molecular origin of DNA-drug specificity in netropsin and distamycin. *Proc. Natl. Acad. Sci. U.S.A.* **1985**, *82*, 1376–1380. (b) Coll, M.; Aymani, J.; van der Marel, G. A.; van Boom, J. H.; Rich, A.; Wang, A. H.-J. Molecular Structure of the Netropsin-d(CGCGATATCGCG) Complex:DNA Conformation in an Alternating AT Segment. *Biochemistry* **1989**, *28*, 310–320. (c) Tabernero, L.; Verdaguer, N.; Coll, M.; Fita, I.; van der Marel, G. A.; van Boom, J. H.; Rich, A.; Aymami, J. Molecular Structure of the A-Tract DNA Dodecamer d(CGCAAATTTGCG) Complexed with the Minor Groove Binding Drug Netropsin. *Biochemistry* **1993**, *32*, 8403–8410. (d) Brown, D. G.; Sanderson, M. R.; Garman, E.; Neidle, S. Crystal Structure of a Berenil-d(CGCAAATTTGCG) Complex. An Example of Drug-DNA Recognition Based on Sequence-dependent Structural Features. *EMBO J. Mol. Biol.* **1992**, *226*, 481–490.

(3) (a) Goodsell, D.; Dickerson, R. E. Isohelical Analysis of DNA Groove-Binding Drugs. *J. Med. Chem.* **1986**, *29*, 727–733. (b) Zasedatelev, A. S. Geometrical correlations useful for design of sequence-specific DNA narrow groove binding ligands. *FEBS Lett.* **1991**, *281*, 209–211. (c) Cory, M.; Tidwell, R. R.; Fairley, T. A. Structure and DNA Binding Activity of Analogues of 1,5-Bis(4-amidinophenoxy)pentane (Pentamidine). *J. Med. Chem.* **1992**, *35*, 431–438.

(4) (a) Pabo, C. O.; Sauer, R. T. Transcription Factors: Structural Families and Principles of DNA Recognition. *Annu. Rev. Biochem.* **1992**, *61*, 1053–1095. (b) Suzuki, M. A framework for the DNA-protein recognition code of the probe helix in transcription factors: the chemical and stereochemical rules. *Structure* **1994**, *2*, 317–326.

(5) (a) Chen, Y.; Lown, J. W. A New DNA Minor Groove Binding Motif: Cross-Linked Lexitropsins. *J. Am. Chem. Soc.* **1994**, *116*, 6995–7005. (b) Blasko, A.; Browne, K. A.; Bruice, T. C. Microgonotropens and Their Interactions with DNA. Structural Characterization of the 1:1 Complex of d(CGCAAATTTGCG)$_2$ and Tren-Microgonotropen-b by 2D NMR Spectroscopy and Restrained Molecular Modeling. *J. Am. Chem. Soc.* **1994**, *116*, 3726–3737. (c) Dwyer, T. J.; Geierstangeer, B. H.; Mrksich, M.; Dervan, P. B.; Wemmer, D. E. Structural Analysis of Covalent Peptide Dimers, Bis(pyridine-2-carboxamidonetropsin)$(CH_2)_{3-6}$, in Complex with 5′-TGACT-3′ Sites by Two-Dimensional NMR. *J. Am. Chem. Soc.* **1993**, *115*, 9900–9906.

(6) Laughon, A. DNA Binding Specificity of Homeodomains. *Biochemistry* **1991**, *30*, 11357–11367.

(7) (a) Kim, J. L.; Nikolov, D. B.; Burley, S. K. Co-crystal of TBP recognizing the minor groove of a TATA element. *Nature* **1993**, *365*, 520–527. (b) Kim, Y.; Geiger, J. H.; Hahn, S.; Sigler, P. B. Crystal structure of a yeast TBP/TATA-box complex. *Nature* **1993**, *365*, 512–527.

(8) Geiersanger, B. H.; Volkman, B. F.; Kremer, W.; Wemmer, D. E. Short Peptide Fragments Derived from HMG-I/Y Proteins Bind Specifically to the Minor Groove of DNA. *Biochemistry* **1994**, *33*, 5347–5355.

(9) Feng, J.; Johnson, R. C.; Dickerson, R. E. Hin Recombinase Bound to DNA: The Origin of Specificity in Major and Minor Groove Interactions. *Science* **1994**, *263*, 348–355.

(10) Dorn, A.; Afflolter, M.; Müller, M.; Gehring, W. J.; Leupin, W. Distamycin-induced inhibition of homeodomain-DNA complexes. *EMBO J.* **1992**, *11*, 279–286.

(11) Chaing, S.-Y.; Welch. J.; Rauscher, F. J.; Beerman, T. A. Effects of Minor Groove Binding Drugs on the Interaction of TATA Box Binding Protein and TFIIA with DNA. *Biochemistry* **1994**, *33*, 7033–7040.

(12) (a) Montgomery, A. B.; Luce, J. M.; Turner, J.; Lin, E. T.; Debs, R. J.; Corkery, K. J.; Brunette, E. N.; Hopewell, P. C. Aerosolised pentamidine as sole therapy for *Pneumocystis carinii* pneumonia in patients with acquired immunodeficiency syndrome. *Lancet* **1987**, *ii*, 480–482. (b) Gazzard, B. G. Pneumocystis carinii pneumonia and its treatment in patients with AIDS. *J. Antimicrob. Chemother.* **1989**, *23*, 67–75. (c) Wispelwey, B.; Pearson, R. D. Pentamidine: A review. *Infect. Control. Hosp. Epidemiol.* **1991**, *12*, 375–381.

(13) (a) Tidwell, R. R.; Jones, S. K.; Geratz, J. D.; Ohemeng, K. A.; Cory, M.; Hall, J. E. Analogues of 1,5-bis(4-amidinophenoxy)-pentane (pentamidine) in the treatment of experimental *Pneumocystis carinii* pneumonia. *J. Med. Chem.* **1990**, *33*, 1252–1257. (b) Jones, S. K.; Hall, J. E.; Allen, M. A.; Morrison, S. D.; Ohemeng, K. A.; Reddy, V. V.; Geratz, J. D.; Tidwell, R. R. Pentamidine analogs in the treatment of experimental Pneumocystis carinii pneumonia. *Antimicrob. Agents Chemother.* **1990**, *34*, 1026–1030.

(14) (a) Edwards, K. J.; Brown, D. G.; Spink, N.; Skelly, J. V.; Neidle, S. Molecular Struture of the B-DNA Dodecamer d(CGCAAATTTGCG)$_2$. An Examination of Propellor Twist and Minor-groove Water Structure at 2.2Å Resolution. *J. Mol. Biol.* **1992**, *226*, 1161–1173. (b) Nunn, C. M.; Jenkins, T. C.; Neidle, S. Crystal Structure of d(CGCGAATTCGCG) Complexed with Propamidine, a Short-Chain Homologue of the Drug Pentamidine. *Biochemistry* **1993**, *32*, 13838–13843.

(15) Dickerson, R. E.; Drew, H. R. Structure of a B-DNA dodecamer: Influence of Base Sequence on Helix Structure. *J. Mol. Biol.* **1981**, *151*, 761–768.

(16) Fox, K. R.; Sansom, C. E.; Stevens, M. F. G. Footprinting studies on the sequence-selective binding of pentamidine to DNA. *FEBS Lett.* **1990**, *266*, 150–154.

(17) Greenidge, P. A.; Jenkins, T. C.; Neidle, S. DNA Minor Groove Recognition Properties of Pentamidine and its Analogs: A Molecular Modeling Study. *Mol. Pharmacol.* **1993**, *43*, 982–988.

(18) Coll, M.; Frederick, C. A.; Wang, A. H.-J.; Rich, A. A bifurcated hydrogen-bonded conformation in the d(A·T) base pairs of the DNA dodecamer d(CGCAAATTTGCG) and its complex with distamycin. *Proc. Natl. Acad. Sci. U.S.A.* **1987**, *84*, 8385–8389.

(19) Spink, N.; Brown, D. G.; Skelly, J. V.; Neidle, S. Sequence-dependent effects in drug-DNA interaction: the crystal structure of Hoechst 33258 bound to the d(CGCAAATTTGCG)$_2$ duplex. *Nucleic Acids Res.* **1994**, *22*, 1607–1612.

(20) Nunn, C. M.; Jenkins, T. C.; Neidle, S. Crystal structure of γ-oxapentamidine complexed with d(CGCGAATTCGCG)$_2$. The effects of drug structural change on DNA minor-groove recognition. *Eur. J. Biochem.* **1994**, *226*, 953–961.

(21) Berman, H. M.; Olson, W. K.; Beveridge, D. L.; Westbrook, J.; Gelbin, A.; Demeny, T.; Hsieh, S.; Srinivasan, A. R.; Schneider, B. The Nucleic Acid Database - A Comprehensive Relational Database of Three-Dimensional Structures of Nucleic Acids. *Biophys. J.* **1992**, *63*, 751–759.
(22) Brünger, A. T.; Kuriyan, J.; Karplus, M. Crystallographic R Factor Refinement by Molecular Dynamics. *Science* **1987**, *235*, 458–460.
(23) Jones, T. A.; Zou, J.-Y.; Cowan, S. W.; Kjeldgaard, M. Improved Methods for Building Models in Electron Density Maps and the Location of Errors in these Models. *Acta Crystallogr.* **1991**, *A47*, 110–119.
(24) Orozco, M.; Laque, F. J. On the Use of AM1 and MNDO Wave Functions to Compute Accurate Electrostatic Charges. *J. Comput. Chem.* **1990**, *11*, 909–923.
(25) Jenkins, T. C.; Lane, A. N.; Neidle, S.; Brown, D. G. NMR and molecular modeling studies for the interaction of berenil and pentamidine with d(CGCAAATTTGCG)$_2$. *Eur. J. Biochem.* **1993**, *213*, 1175–1184.
(26) Nicholls, A.; Sharp, K.; Honig, B. *Protein Struct., Funct., Genet.* **1991**, *11*, 281–296.
(27) Lavery, R.; Sklenar, H. The Definition of Generalized Helicoidal Parameters and of Axis Curvature for Irregular Nucleic Acids. *J. Biomol. Struct. Dyn.* **1988**, *6*, 63–91.

JM950079W